References

Baz, A., Iman, K. & McCoy, J. 1990. The dynamics of helical shape memory actuators, *Journal of Intelligent Material Systems and Structures,* Vol. 1, January, p. 105-133.

Braun, D. 1980. Development of anti-resonance force isolators for helicopter vibration reduction, *Sixth European Rotocraft and Powered Lift Aircraft Forum,* Bristol, England, September 16-19, Paper no. 18, p. 1-17.

Bo, Z. & Lagoudas, D.C. 1995. A unified thermodynamic constitutive model and finite element analysis of active metal matrix composites, *Active Materials and Smart Structures,* SPIE Vol. 2427, p. 276-288.

Brennan, M.J., Elliot S.J., Long, T. 1996. Automatic control of multiple vibration neutralisers, *Proceedings of Inter-noise,* Vol 96. p.1597-1602.

Brennan, M.J. 2000. Actuators for active vibration control – Tunable resonant devices, *Applied Mechanics and Engineering,* Vol. 5, No. 1, p.63-74.

Carlson, J.D. & Weiss, K.D. 1995. Magnetorheological materials based on alloy particles, *U.S. Patent 5,382,373.*

Chen, Q. 1999. Development of mesoscale actuator devices with microinterlocking mechanism, *Mechanical and Aerospace Engineering Department, University of California.*

Davis, L.C. 1999. Model of magnetorheological elastomers, *Journal of Applied Physics,* Vol. 85, Nr. 6, p. 3348 – 3351.

Desjardins, R.A. & Hooper, W.E. 1976. Rotor isolation of the hingeless rotor B0-105 and YUH-61A helicopters, *2nd European Rotorcraft and Powered Lift Aircraft Forum,* Buckeburg, F.R.G., September, Paper no. 13, p. 1-13.

Desjardins, R.A. & Hooper, W.E. 1980. Antiresonant rotor isolation for vibration reduction, *Journal of the American Helicopter Society,* Vol. 25, no. 3, July, p.46-55.

Dorf, R.C. & Bishop, R.H. 1995. *Modern Control Systems,* Addison-Wesley Publishing Company, Inc.

Du Plooy, N.F., 1999. The development of a vibration absorber for vibrating screens, *M. Eng, University of Pretoria.*

Duerig, T.W., Melton, K.N., Stockel, D. & Wayman, C.M. 1990. *Engineering Aspects of Shape Memory Alloys,* Butterworth-Heinemann Ltd.

Dyke, S.J., Spencer Jr., B.F., Sain, M.K.& Carlson, J.D. 1996. Modeling and control of magnetorheological dampers for seismic response reduction, *Smart Materials and Structures*, Vol. 5, August, p. 565-575.

Feng, Z.C. and Li, D.Z. 1996. Dynamics of a mechanical system with a shape memory alloy bar, *Journal of Intelligent Material Systems and Structures,* Vol 7 July, p.399-410.

Flanneley, W.G. 1966. The dynamic anti-resonant vibration isolator, *22nd Annual AHS National Forum,* Washington, p.153-158.

Flatau, A.B., Dapino, M.J., Calkins, F.T. 1998. High bandwidth tunability in a smart vibration absorber, *SPIE Smart Structures and Materials Conf,* Paper #3329-19/3327-42.

Flower, W.C. 1985. Understanding hydraulic engine mounts for improved vehicle noise, vibration and ride qualities, Technical report 850975, *Society of Automotive Engineers.*

Ford, D.S., Hebda, D.A. & White, S.R. 1995. Constitutive and transformation behaviour of TWSM nitinol, *Active Materials and Smart Structures,* SPIE Vol. 2427, p.218-233.

Fosdick, R. & Ketema, Y. 1998. A thermoviscoelastic dynamic vibration absorber, *Journal of Applied mechanics,* Vol. 65, March, p.17-24.

Franchek, M.A., Ryan, M.W., Bernhard, R.J. 1995. Adaptive passive vibration control, *Journal of Sound and Vibration,* Vol. 189, No. 5, p.565-585.

Ginder, J.M., Nichols, M.E., Elie, L.D., Clark, S.M. 2000. Controllable-stiffness components based on magnetorheological elastomers, *Proceedings of SPIE Smart Structures and Integrated Systems,* Vol. 3985, March, p.418-425.

Ginder, J.M., Nichols, M.E., Elie, L.D., Tardiff, J.L. 1999. Magnetorheological elastomers: Properties and applications, *SPIE Conference on Smart Materials Technologies,* Vol. 3675 p. 131 – 138.

Halwes, D.R. & Simmons, W.A. 1980. Vibration suppression system, *U.S. patent no. 4,236,607.*

Halwes, D.R. 1981. Total main rotor isolation system analysis, Bell helicopter textron, *NASA Contractor Report No. 165667.* Langley Research Center, Hampton, Virginia, June.

Herakovic, N. 1998. Smart actuators in robotics, *University of Ljubljana*

Hodgson, D.A. & Duclos, T.G. 1991. Vibration isolator with electrorheological fluid controlled dynamic stiffness, *U.S. Patent 5,029,823*

Hodgson, D.E., Wu, M.H. & Biermann, R.J. 1999. Shape memory alloys, *http://www.sma-inc.com/SMAPaper.html*

Hooker, M.W. 1997. Properties and performance of RAINBOW piezoelectric actuator stacks, *Smart Materials and Structures : Industrial and Commercial Applications of Smart Structures Technologies*, Proc. SPIE vol. 3044, p. 413-420.

Janker, P. 1998. Development of high-performance piezoelectric actuators for transport systems, *Daimler-Benz AG Research and Technology*

Jolly, M.R., Carlson, J.D., Munoz, B.C., Bullions, T.A. 1996a. The magnetoviscoelastic response of elastomer composites consisting of ferrous particles embedded in a polymer matrix, *Journal of Intelligent Material Systems and Structures,* Vol. 7 p. 613 – 622.

Jolly, M.R., Carlson, J.D., Munoz, B.C. 1996b. A model of the behaviour of magnetorheological materials, *Smart Material Structures,* Vol. 5 p. 607-614.

Ketema, Y. 1998. A viscoelastic dynamic vibration absorber with adaptable supression band: A feasibility study. *Journal of Sound and Vibration,* Vol. 216, No. 1, p.133-145.

Liang, C. & Rogers, C.A. 1993. Design of shape memory alloy springs with applications in vibration control, *Journal of Vibration and Acoustics,* Vol. 115, January, p. 129-135.

Lin, R. 1996. Shape memory alloys and their applications, *http://www.stanford.edu/~richlin1/sma/sma.html*

Lin, H.C., Wu, S.K. & Yeh, M.T. 1993. Damping characteristics of TiNi shape memory alloys. *Metallurgical Transactions,* Vol. 24A, October, p. 1993-2189.

Longbottom, C.J. & Rider, M.J.D.E. 1987. A self-tuning vibration absorber, *UK Patent,* GB 2189573 B, London.

Mashinostroeniya, V. 1987. Variable-stiffness springs with packs of cylindrical panels, *Soviet Engineering Research,* Vol. 67, Issue 4, p. 44-47.

Maw, A.N. 1991. The design of resilient mounting systems to control machinery noise in buildings. *Plastics, Rubber and Composites Processing and Applications*, Vol. 18, No. 1, p.9-16.

McKeown, W.L., Smith, M.R. & Stamps, F.B. 1995. Hydraulic inertial vibration isolator, *U.S. Patent 5,439,082*

Meghdari, A., Jafarian, M., Mojarrad, M. & Shahinpoor, M. 1993. Exploring artificial muscels as actuators for artificial hands, *Intelligent Structures, Materials and Vibrations,* ASME, Vol. 58, p. 21-26.

Monkman, G.J. 2000. Advances in shape memory polymer actuation, *Mechatronics,* Vol. 10, p. 489-498.

Nagem, R.J., Madanshetty, S.I., Medhi, G. 1997. An electromechanical vibration absorber, *Journal of Sound and Vibration,* Vol. 200, no. 4, p.551-556.

Ogontz Corporation. 1998. The wax actuator, *http://www.ogontz.com/html/wax_tech.html*

Onoda, J., Sano, T., Kamiyama, K. 1992. Active, passive, and semiactive vibration supression by stiffness variation, *AIAA Journal,* Vol. 30, No. 12, December, p. 2922-2929.

Rao, S.S. 1995. *Mechanical Vibrations,* 3rd Edition, New York: Addison Wesley.

Raw, S. 1999. Ergonomic hand-grip for attenuating vibrations in hand-held power tools, *Health an Safety,* May.

Ribakov, Y. & Gluck, J. 1998. Optimal design of base isolated active controlled MDOF structures, *ISMA 23.*

Rita, A.D., McGarvey, J.H., Jones, R. 1976. Helicopter rotor isolation utilizing the dynamic antiresonant vibration isolator. *32nd Annual AHS National Forum,* Washington, May, p. 22-29.

Segalman, D.J., Parker, G.G. & Inman, D.J. 1993. Vibration suppression by modulation of elastic modulus using shape memory alloy, *Intelligent Structures, Materials and Vibrations,* ASME, Vol. 58, p. 1-5.

Seto, K. & Yamanouch, M. 1978. On the effect of a variable stiffness-type dynamic absorber with eddy-current damping, *Bulletin of the JSME*, Vol. 21, No. 160, October, p.1482-1489.

Siler, D. & Demoret, K.B. 1996. Variable stiffness mechanisms with SMA actuators, *SPIE,* Vol. 2721, p. 427-435.

Simrit. Standard Catalogue Standard Range Part A, *Freudenberg*

Smith, K.E. 1991. Smart tuned mass dampers, *Proceedings of ADPA/AIAA/ASME/SPIE Conference on Active Materials and Adaptive Structures.*

Smith, M.R. & Stamps, F.B. 1995. Vibration isolation system, *U.S. Patent 5,435,531*

Smith, M.R. & Stamps, F.B. 1998. Vibration isolation system, *U.S. Patent 5,788,029*

Stalmans, R. & Van Humbeeck, J. 1995. Shape memory alloys: Functional and smart, *Smart Materials and Technologies – Sensors, Control Systems and Regulators,* October, Prague, Czech Republic, http://www.mtm.kuleuven.ac.be/Research/ADAPT/publicat/ShapeMemory/smatext.htm.

Sun, J.Q., Jolly, M.R. & Norris, M.A. 1995. Passive, adaptive and active tuned vibration absorbers – A Survey. *Transactions of the ASME*, Vol. 117, June, p.234-242.

Tentor, L.B. & Wicks, A.L. 2000. Electromagnetic tuned dynamic vibration absorber – Theoretical foundations, *IMAC 18,* San Antonio, February, p.440-447.

Theron, N.J. 2002. Some notes on first order systems, *University of Pretoria,* February.

Von Flotow, A.H., Beard, A., Bailey, D. 1994. Adaptive tuned vibration absorbers: Tuning laws, tracking agility, sizing, and physical implementations, *Noise-Con 94,* May, p. 437-454.

Walsh, P.L., Lamancusa, J.S. 1992. A variable stiffness vibration absorber for the minimisation of transient vibrations, *Journal of Sound and Vibration,* Vol. 158, No. 2, p.195-211.

Williams, K.A., Chiu, G.T.-C., Bernhard, R.J. 1999. Passive-adaptive vibration absorbers using shape memory alloys, *Proceedings of SPIE Smart Structures and Integrated Systems,* Vol. 3668, March, p.630-641.

Williams, K.A., Chiu, G.T.-C., Bernhard, R.J. 2000. Controlled continuous tuning of an adaptively tunable vibration absorber incorporating shape mamory alloys, *Proceedings of SPIE Smart Structures and Integrated Systems,* Vol. 3984, March, p.564-575.

Witting, P.R. & Cozzarelli, F.A., 1995. Experimental determination of shape memory alloy constitutive model parameters, *Active Materials and Smart Structures,* SPIE Vol. 2427, p. 260-275.

Yu, Y., Naganathan, N.G. & Dukkipati, R.V. 2000. A literature review of automotive vehicle engine mounting systems, *Mechanisms and Machinery Theory,* Vol. 36, p. 123-142.

APPENDIX A

Measurement of spring stiffness and damping

A.1 Theory

Most springs have an amount of structural damping. The only springs without it would probably be magnetic springs or other non-contact type springs. All the springs considered in this study had structural damping and it was necessary to measure this damping very accurately.

Structural damping is a phenomenon where if the spring is excited with sinusoidal excitation, the displacement of the spring and the force transmitted are not in phase as is expected. Furthermore, the force is leading the displacement, which is even more unexpected. Structural damping is usually given as the loss factor η. The loss factor can be related to other constants with the following equations:

$$\eta = \frac{h}{k} \tag{A.1}$$

$$h = c\omega \tag{A.2}$$

Another way in which structural damping is sometimes expressed is tan δ. This can be related to η with the following equation:

$$\eta = \tan\delta = \tan\left(\phi_{Force} - \phi_{Displacement}\right) \tag{A.3}$$

Where ϕ_{Force} and $\phi_{Displacement}$ are the phase angles of the force and displacement signals.

Therefore, it is possible to relate any of the constants to the loss factor, and therefore any constant can be determined out of experimental results. The most obvious way to determine the loss factor is to determine the phase shifts of the force and displacement signals and to determine tan δ. With sinusoidal excitation the force and displacement signals are sine waves and a fit can easily be obtained.

A sine wave is described with the following equation:

$$y(t) = A\sin\left(\omega t + \phi\right) \tag{A.4}$$

A least squares fit can be done to the measured force and displacement signals by substituting the known frequency into ω and to assign A and ϕ as the two variables. Therefore an amplitude A and a phase shift ϕ will be determined for the force signal and the displacement signal. From that the loss factor of the spring can be determined with equation (A.3) and the stiffness of the spring can be determined with:

$$k = \frac{f_{x=X}}{A_x} \tag{A.5}$$

Where $f_{x=X}$ is the force at maximum displacement and A_x is the amplitude of the displacement.

Figure A. 1 explains the whole concept.

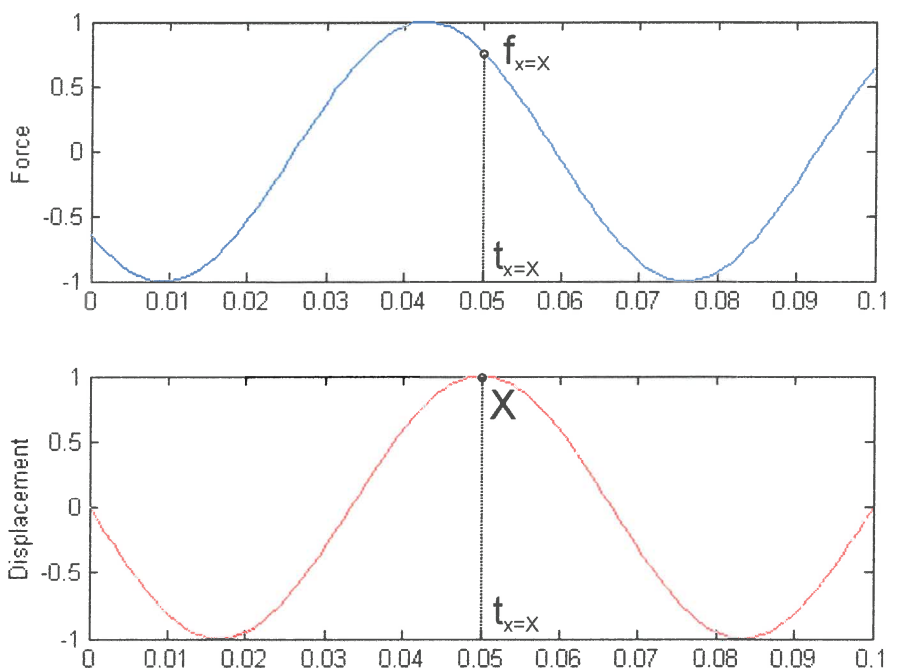

Figure A. 1 Force and displacement time signals

Another method of determining the stiffness and damping, is by using the hysteresis loop method and determining the viscous damping constant *c* and then translating it back to the loss factor.

A hysteresis loop is obtained when the force and displacement are plotted against each other on the same graph. Due to the phase shift, an ellipse is formed. Figure A. 2 explains the concept.

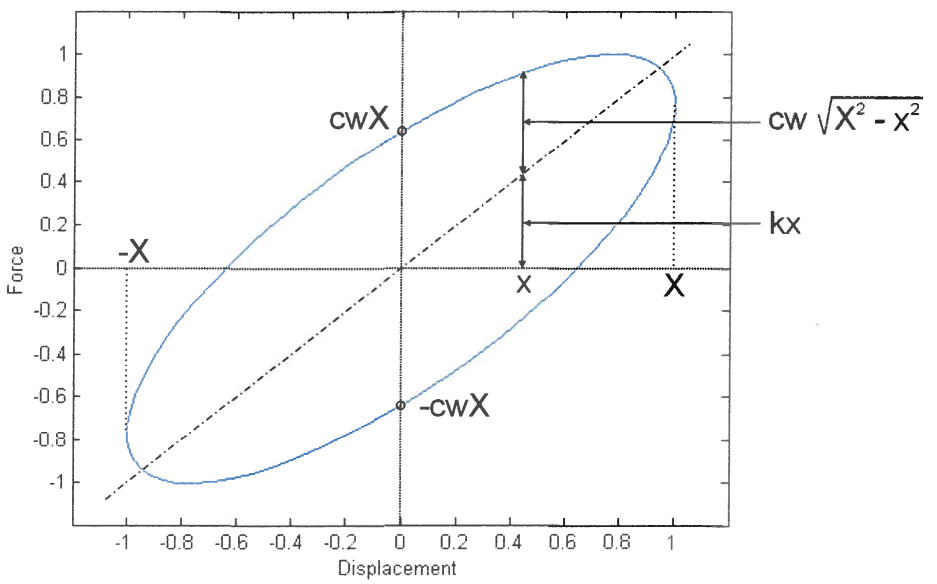

Figure A. 2 Hysteresis loop

The equation of the ellipse can be derived as follow (Rao, 1995):

Consider a spring and viscous damper. The force needed for a certain displacement is:

$$F = kx + c\dot{x} \tag{A.6}$$

For harmonic motion of frequency ω and amplitude X:

$$x(t) = X \sin \omega t \tag{A.7}$$

Combining the equations give:

$$\begin{aligned} F(t) &= kX \sin \omega t + cX\omega \cos \omega t \\ &= kx \pm c\omega\sqrt{X^2 + (X \sin \omega t)^2} \\ &= kx \pm cw\sqrt{X^2 - x^2} \end{aligned} \tag{A.8}$$

From experimental results, the hysteresis loop can be produced. A least squares fit can be done on the hysteresis loop with equation (A.8) and the stiffness k and the

viscous damping constant c can be determined. The loss factor can then be determined with equations (A.2) and (A.1).

A.2 Practical considerations

If the theory is considered, one important practical aspect that comes forward is accurate measurement, especially as far as the phase is concerned.

Let us evaluate the normal laboratory experiment with the measurement transducers that are usually used for these measurements as depicted in Figure A. 3.

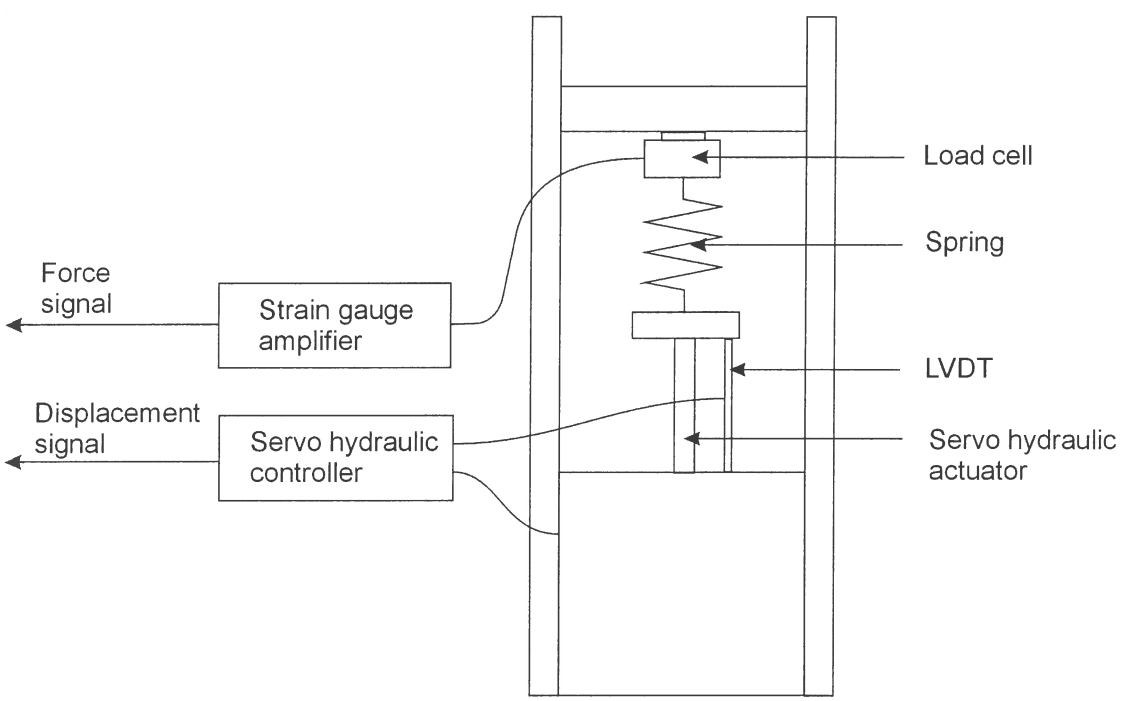

Figure A. 3 Experimental measurement system

As far as the amplitude of the signals are considered, there are no problem with this experimental measurement technique because the transducers are usually calibrated and should be accurate. If the phase of the signals is considered, there seems to be some amount of confusion. The reason for this is that the strain gauge amplifier and servo hydraulic controller with its LVDT amplifier are seen as black boxes and it is unknown what exactly is happening inside them. To try and find out what exactly is

done to the signals is also a fruitless exercise. If the basic principal of strain gauge (or LVDT) amplifiers is considered, it comes to light that all of them have some sort of filter in them. These filters' characteristics are unknown and can sometimes be altered by the user by setting cut-off frequencies etc. Let us consider the characteristics of a 4th order Butterworth filter shown in Figure A. 4.

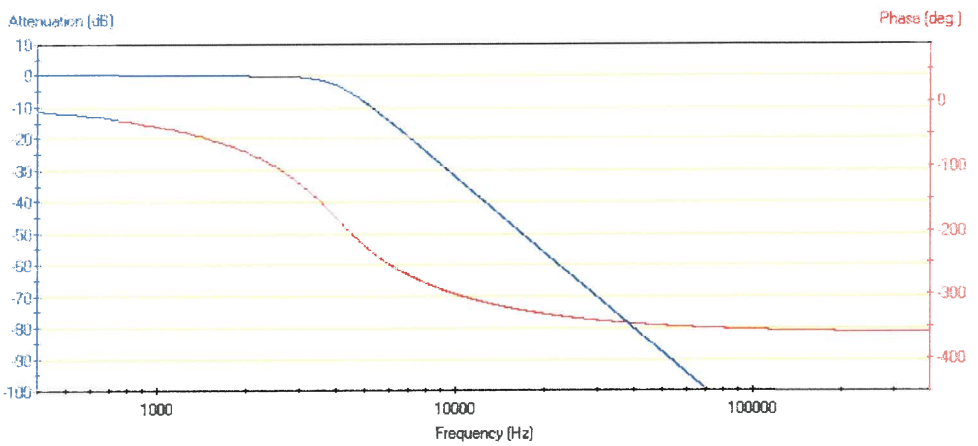

Figure A. 4 Characteristics of a 4th order Butterworth filter

It can be seen that the amplitude is not altered below the cut off frequency, but that is certainly not the case with the phase. There is a phase shift from 0 Hz onwards and it is also not constant over frequency, not even in a certain region. This causes a problem for damping measurements because it is exactly this phase shift that is measured to determine the amount of damping. A filter would therefore alter the measured damping considerably.

It is therefore noted that the most widely accepted way of measuring force and displacement yielded the wrong values and that a very specific measuring technique must be used to accurately measure the damping of a spring. The only way in which this way of measuring could be accurate, is if the phase shift of the strain gauge amplifier and the LVDT amplifier is the same. It is possible, especially when the strain gauge amplifier in the controller is used for the load cell instead of an external amplifier as shown in the sketch, but it must first be confirmed. There could still be a phase shift due to the internal working mechanism of an LVDT, which would not be present in the strain gauges in the load cell.

To accurately measure the damping of a spring, there are two possibilities. Either transducers with zero phase shift must be used, or the phase shift of the two transducers must be exactly the same. The first option is not practically possible, so the phase shift of the transducers must be kept exactly the same. As mentioned above, an LVDT could have some phase shift internally so it will not be an option. The only way to be sure that the two transducers will respond identically is if both worked on the same principle. Therefore a strain gauge displacement transducer was used for the measurements. The load cell and strain gauge displacement transducer were amplified with the same HBM MGC strain gauge amplifier with both channels set to a 400 Hz Bessel filter. This would ensure exactly the same phase shift on both transducers and would therefore yield an accurate damping value.

APPENDIX B

Determining separation force

B.1 Separation force

The separation force is defined as the force needed to keep the two leaf springs apart in the centre. In FEM tests, the stiffness of the individual springs is known and it is necessary to determine the separation force from that.

Consider a single spring with the following characteristic:

Table B. 1 Spring characteristics

Displacement	Force
1 mm	100 N
2 mm	220N
3 mm	360 N
4 mm	520 N
5 mm	700 N

Now it is desirable to determine the stiffness of a compound spring separated by different amounts and also the separation force needed to separate the two springs. This can be done as follows:

Let us assume the compound spring is displaced 1mm upwards in the centre from its neutral position for different separation distances. The following table can then be compiled:

Table B. 2 Spring forces

Separation	Force on top spring	Force on bottom spring
2 mm	220 N	0 N
4 mm	360 N	100 N
6 mm	520 N	220 N
8 mm	700 N	360 N

Let us consider the situation graphically in Figure B. 1.

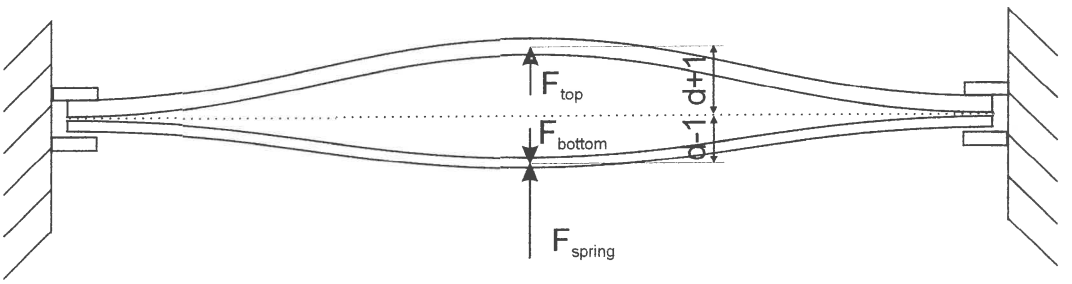

Figure B. 1 **Separation forces**

The actuator is located between the two springs and therefore the separation force will be the same on the two springs. In the case shown in Figure B. 1 it will be equal to the force on the top spring. The stiffness of the compound spring will be the spring force divided by the displacement of the spring (1 mm). The resultant force on the bottom spring must be F_{bottom}. Therefore the spring force will be:

$$F_{spring} = F_{separation} - F_{bottom} = F_{top} - F_{bottom} \tag{B.1}$$

If the above tables are extended the following values will be obtained:

Table B. 3 **Stiffness of spring**

Separation	Stiffness	Separation Force
2 mm	220 000 N/m	220 N
4 mm	260 000 N/m	360 N
6 mm	300 000 N/m	520 N
8 mm	340 000 N/m	700 N

In this way it is not necessary to measure separation force because it can be calculated from the stiffness of a single spring.

APPENDIX C

Stepper motor

A stepper motor consists of a magnetic rotor and a lot of windings on the outer stator. The windings on the outside are usually arranged in groups of four so that the groups alternate as you go round. It is illustrated graphically in Figure C. 1.

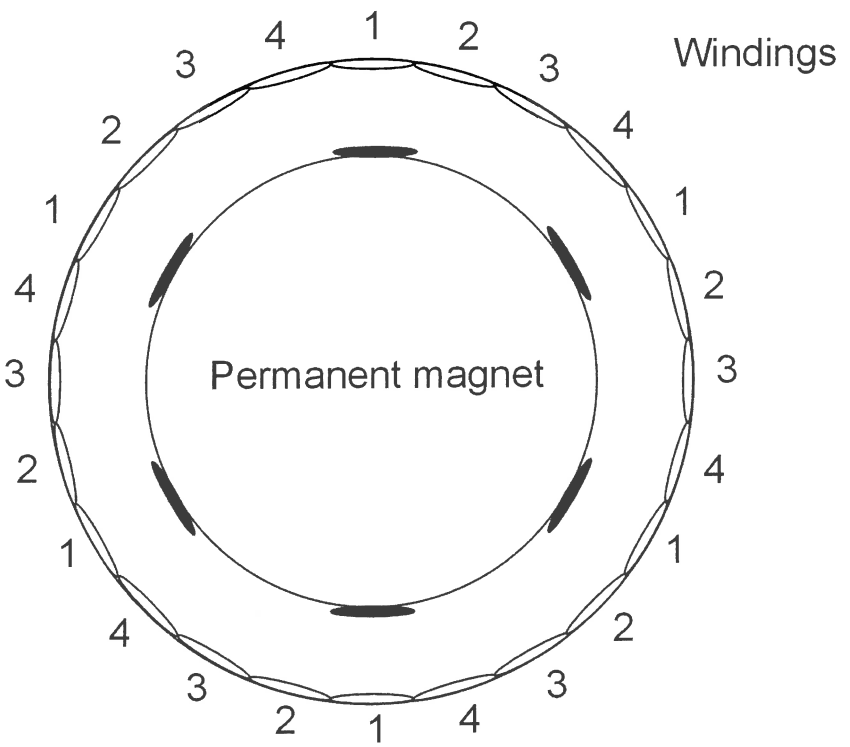

Figure C. 1 Working of a stepper motor

When the first group of windings are activated, all the windings with the number 1 are energised and the permanent magnet is pulled into the orientation as shown above. To let the motor turn 1 step clockwise, the second group of windings are energised so that the permanent magnet will be pulled one step clockwise so that all its poles will be pointing to a number 2 winding. All stepper motors work like this with the only difference being the total number of steps per revolution. This will off course always be a multiple of 4 and common values are 48 or 72 steps per revolution.

With this concept understood, it can be seen that it is very easy to control the motor accurately. To let the motor rotate clockwise, the coils must be energised as follows:

Table C. 1 Clockwise rotation

Step	Coil 1	Coil 2	Coil 3	Coil 4
1	1	0	0	0
2	0	1	0	0
3	0	0	1	0
4	0	0	0	1
5	1	0	0	0
6	0	1	0	0

For anticlockwise movement, the order will be as follows:

Table C. 2 Anticlockwise rotation

Step	Coil 1	Coil 2	Coil 3	Coil 4
1	1	0	0	0
2	0	0	0	1
3	0	0	1	0
4	0	1	0	0
5	1	0	0	0
6	0	0	0	1

It is also possible to use sub-steps to let the motor turn very slowly, but accurately. This can be done as follows:

Table C. 3 Sub-step rotation

Step	Coil 1	Coil 2	Coil 3	Coil 4
1	1	0	0	0
2	1	1	0	0
3	0	1	0	0
4	0	1	1	0
5	0	0	1	0
6	0	0	1	1

When two adjacent coils are energised, the permanent magnet will stop in-between the coils and that is called a sub-step. Sub-steps are only used while the motor is turning and must not be used to keep the motor stationary.

The last utility that can be used is high torque rotation. It can be achieved as follows:

Table C. 4 High torque rotation

Step	Coil 1	Coil 2	Coil 3	Coil 4
1	1	1	0	0
2	0	1	1	0
3	0	0	1	1
4	1	0	0	1
5	1	1	0	0
6	0	1	1	0

Because two coils are energised each time, the force on the permanent magnet is increased and results in a higher torque during rotation.

A very important thing to remember about stepper motors is that they can and will slip if the torque required is too large. This results in a loss of position and usually causes problems. Therefore it is important to ensure that the required torque does not exceed the capabilities of the motor.

To control a stepper motor, some sort of controller or driver is obviously necessary. There are two possibilities, a stepper motor driver or using a computer directly. A stepper motor driver is usually used when more than two stepper motors are used. The reason for this is that it is much cheaper and easier to use a computers parallel port to directly control the coils of the stepper motor. The problem is that there are only 8 channels on a parallel port and therefore only two motors can be controlled. A stepper motor driver uses a serial link to a computer that sends the direction and number of steps for each motor to the controller and the controller does the rest by activating the coils in the correct order. These controllers are quite expensive and are

not easily obtainable, so because only one motor needed to be controlled, the parallel port of a computer was used to do the control.

To control one motor, only 4 channels on the parallel port were used, one for each group of windings. The parallel cannot supply the necessary current to drive the motor, so some kind of driver must be used to supply the current. This driver must have at least 4 channels and must be able to supply the required current. A ULN 2003 transistor array IC was used. It is a 7-channel driver and can supply 0.5 A current in total. It can be triggered directly from the parallel port and no other components are required. LED's were added on the 4 channels to indicate which channels are active. The IC has to be supplied with external power to drive the motor. The circuit is depicted in Figure C. 2.

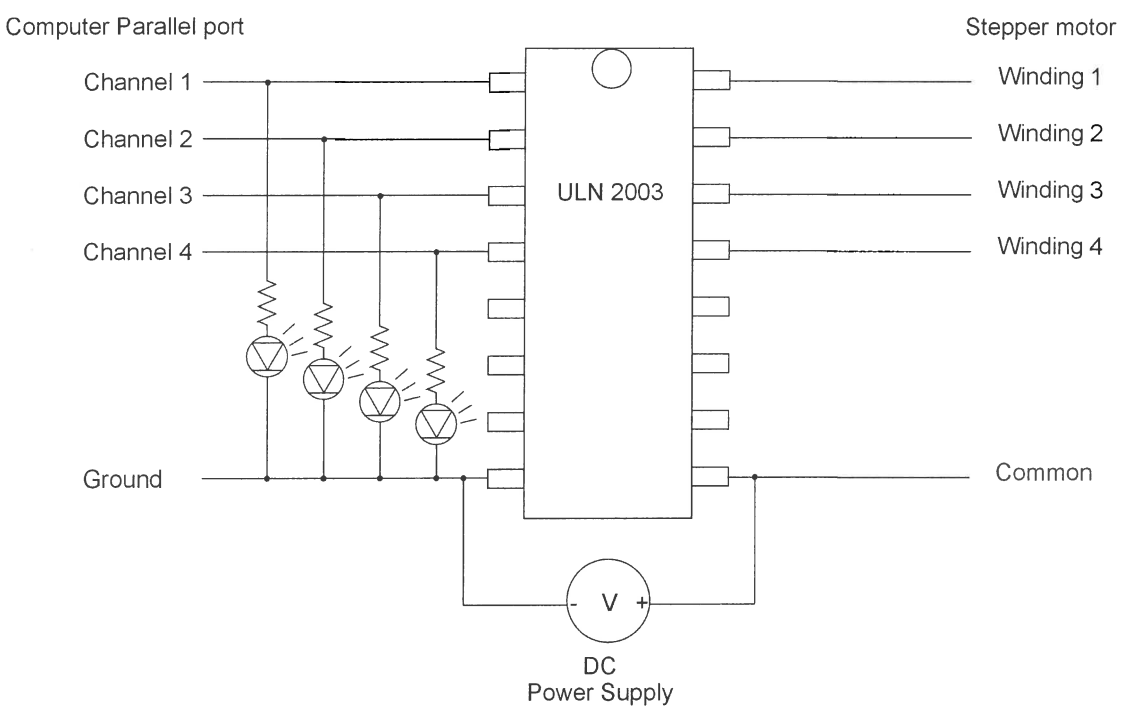

Figure C. 2 Stepper motor driver

If the stepper motor itself is considered, there are usually 6 wires of different colours. The reason for the 6 wires is that 2 sets of windings are connected to the same ground or common. Therefore a multimeter can be used to determine the layout of the wires. The two common wires can be connected to the common on the circuit above and the

other wires to the winding connections. If the wires are connected in the wrong order, the motor will not turn continuously, but jump around.

Once the motor is connected, a Matlab program downloaded from the Internet (http://www.isibrno.cz/~ivovi/matlab.htm) allows you to give output to the parallel port of the computer and the stepper motor can be controlled. To do angular position control, the number of steps per revolution of the motor must be counted and then the angle per step calculated. Once the current position of the motor is known, it can be positioned in any way by letting it move the correct number of steps.

APPENDIX D

Isolator test results

D.1 Transmissibility without water

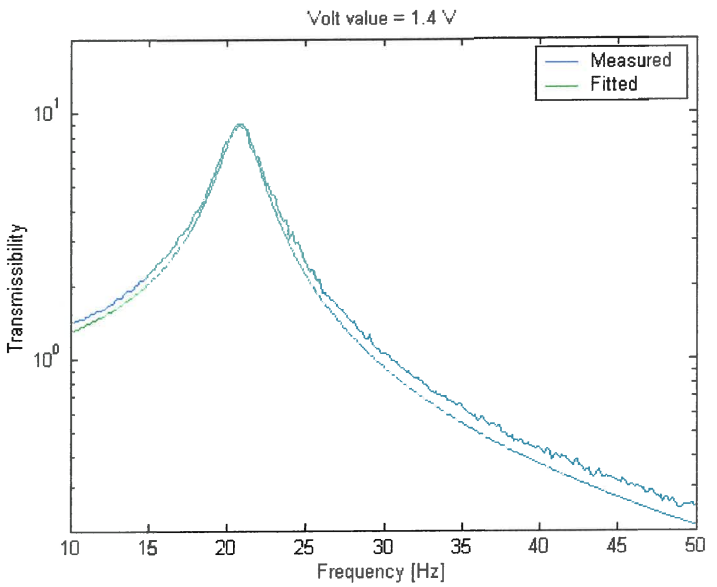

Figure D. 1 **Transmissibility – 1.4 V**

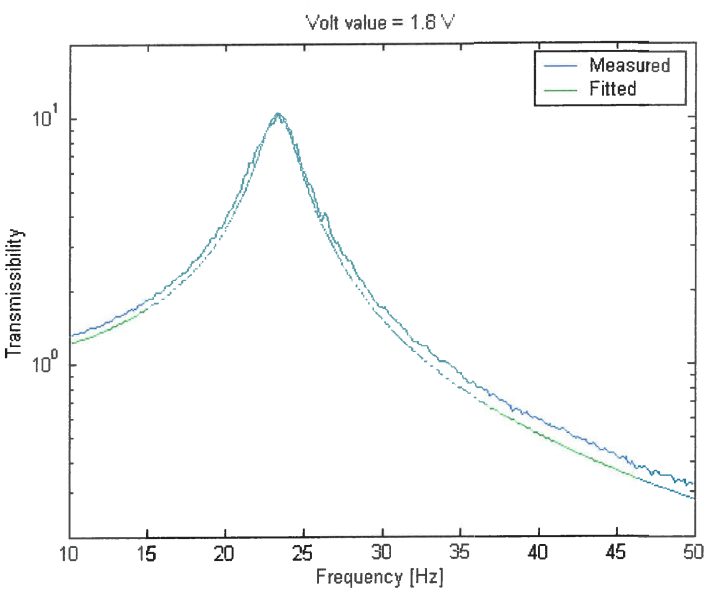

Figure D. 2 **Transmissibility – 1.8 V**

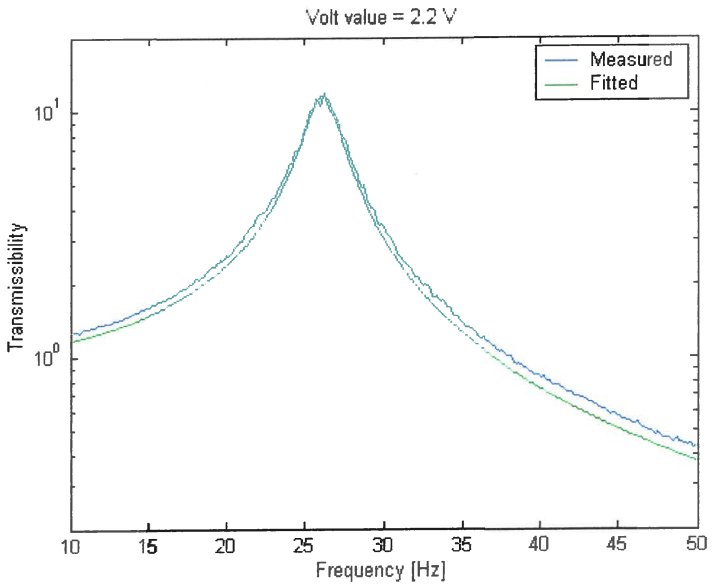

Figure D. 3 Transmissibility – 2.2 V

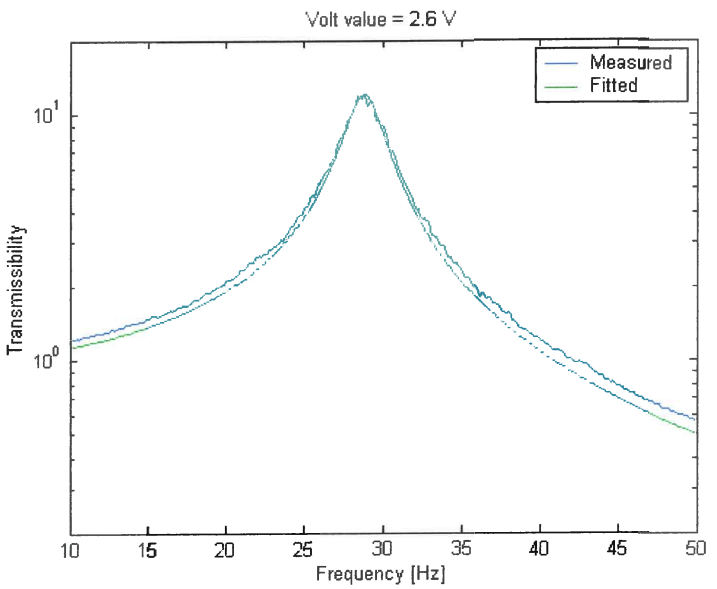

Figure D. 4 Transmissibility – 2.6 V

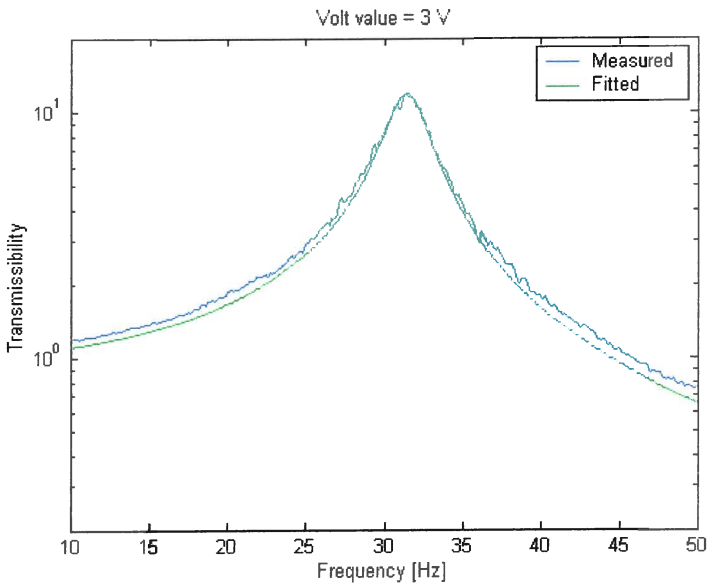

Figure D. 5 Transmissibility – 3.0 V

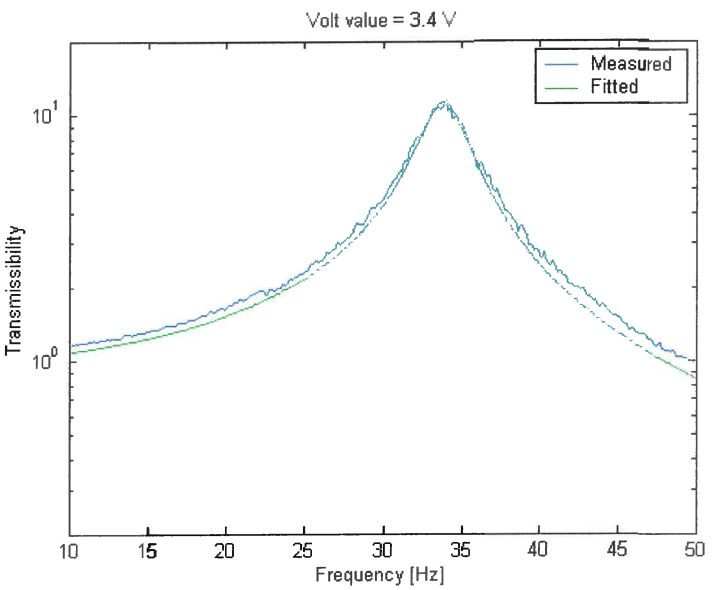

Figure D. 6 Transmissibility – 3.4 V

D.2 Transmissibility with water

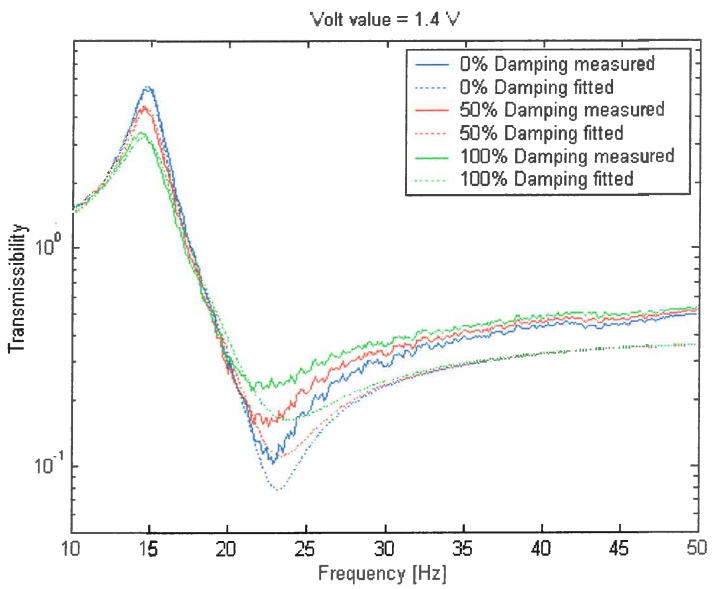

Figure D. 7 Transmissibility – 1.4 V

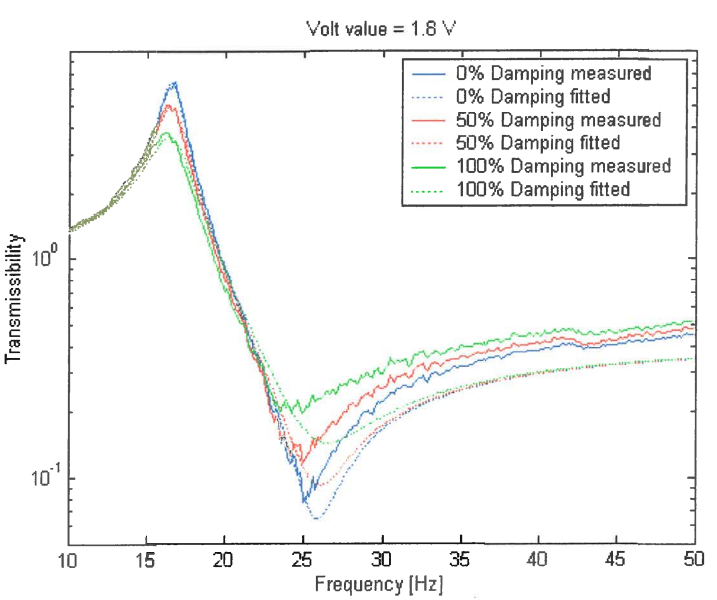

Figure D. 8 Transmissibility – 1.8 V

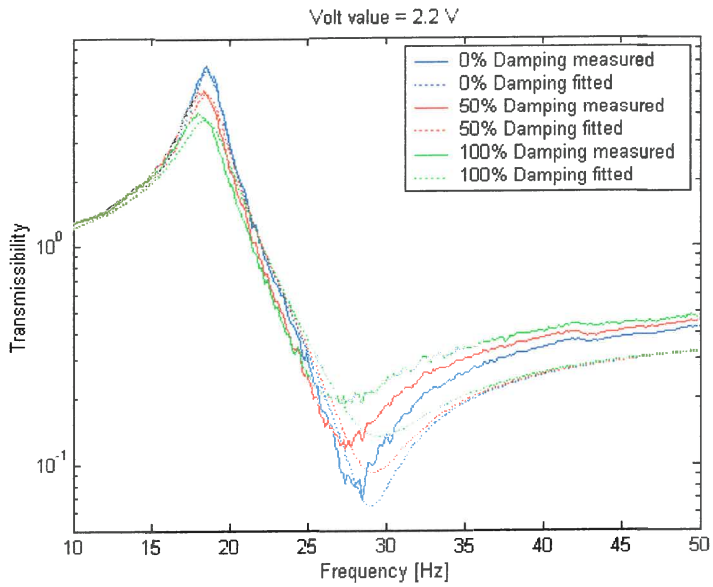

Figure D. 9 **Transmissibility – 2.2 V**

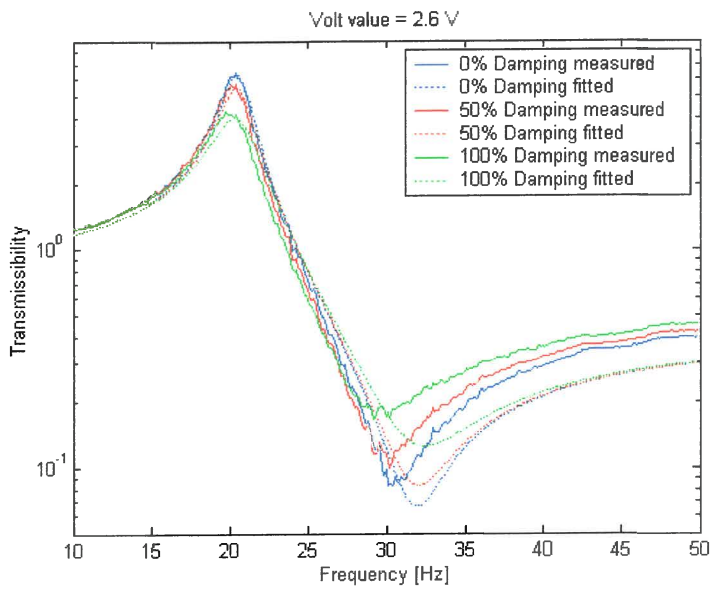

Figure D. 10 **Transmissibility – 2.6 V**

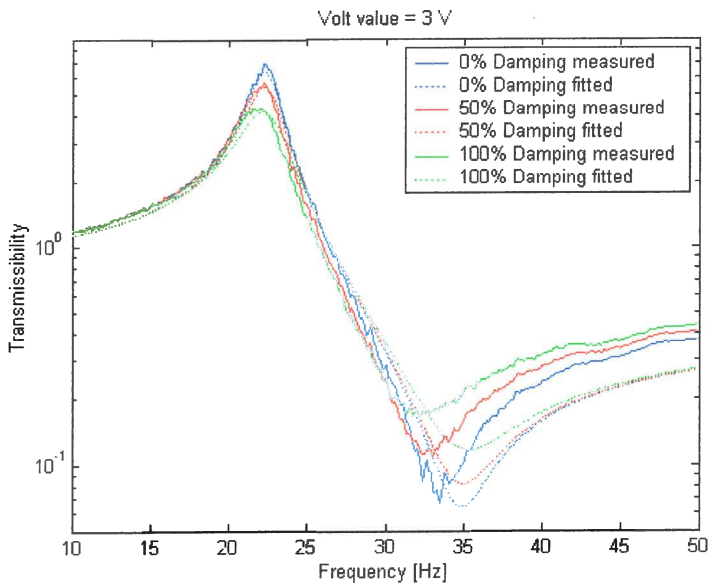

Figure D. 11 Transmissibility – 3.0 V

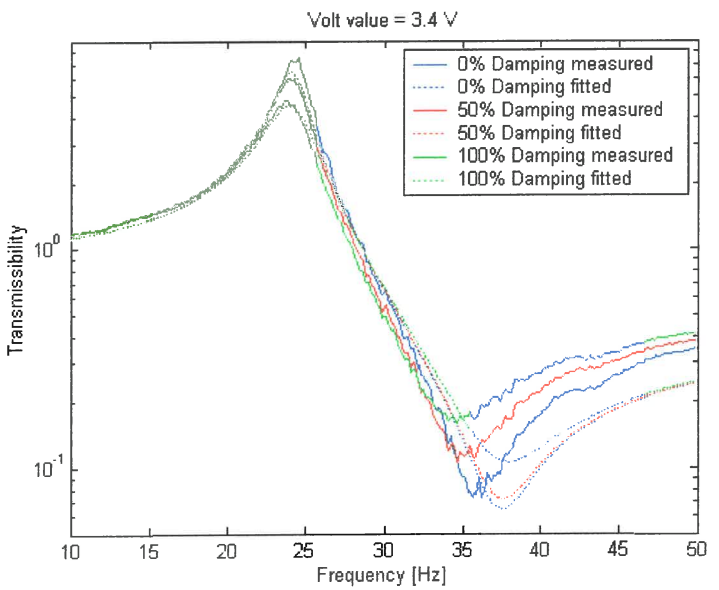

Figure D. 12 Transmissibility – 3.4 V

D.3 Effect of damping

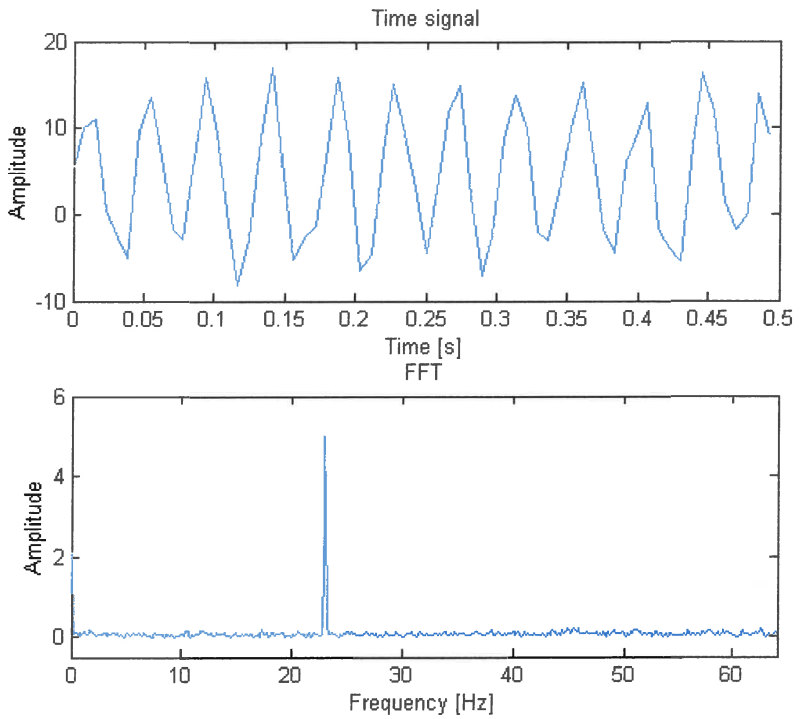

Figure D. 13 Theoretical input signal with medium noise levels

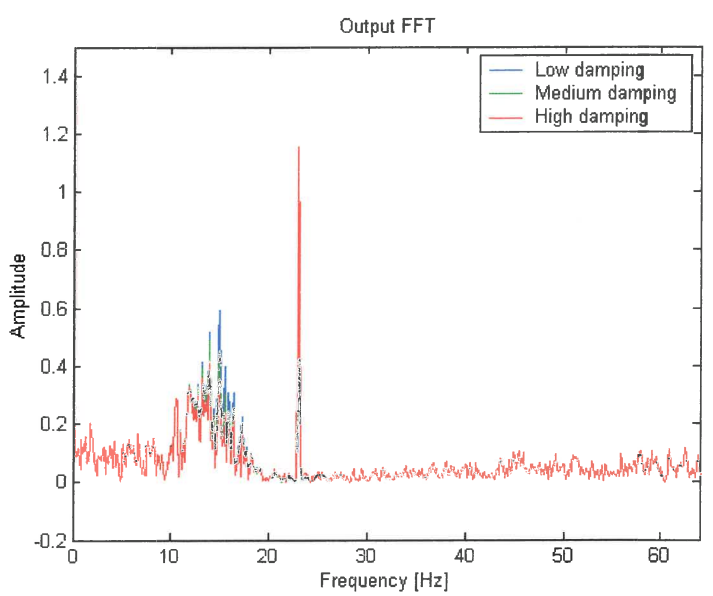

Figure D. 14 Output FFT with medium noise levels

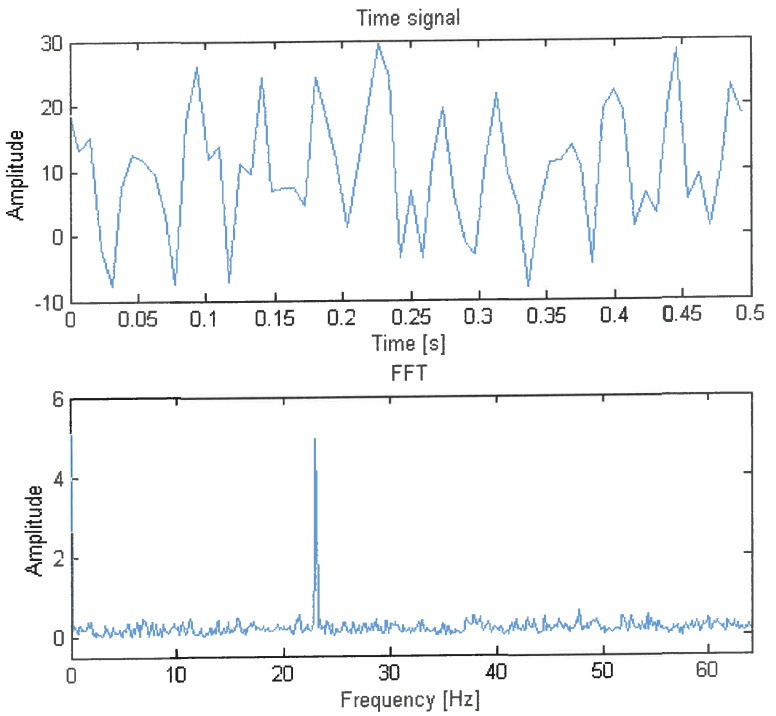

Figure D. 15 **Theoretical input signal with high noise levels**

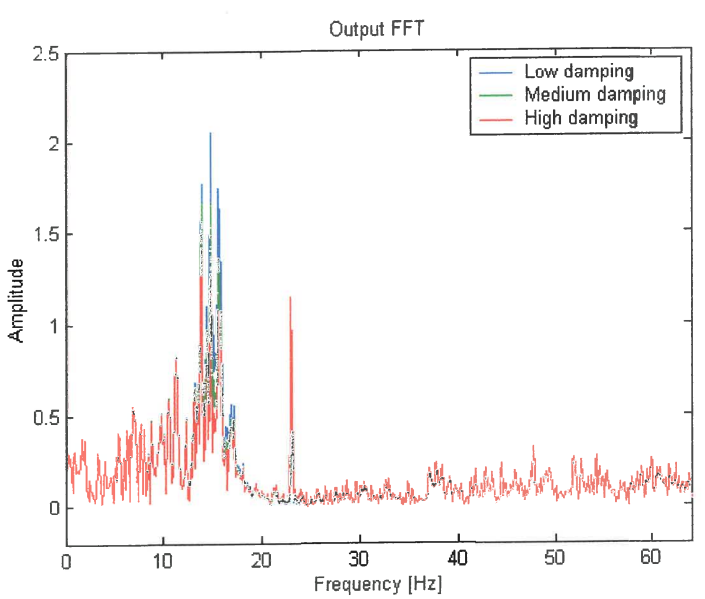

Figure D. 16 **Output FFT with high noise levels**